Macromolecules

ARTICLE

pubs.acs.org/Macromolecules

Microphase and Macrophase Separations in Binary Blends of Diblock Copolymers

Zhiqiang Wu, Baohui Li,* Qinghua Jin, and Datong Ding

School of Physics and Key Laboratory of Functional Polymer Materials of Ministry of Education, Nankai University, Tianjin 300071, China

An-Chang Shi*

Department of Physics and Astronomy, McMaster University, Hamilton, Ontario L8S 4M1, Canada

ABSTRACT: Phase behavior of blends of two AB diblock copolymers, with the long one at relatively strong segregation, is studied using the self-consistent field theory, focusing on the effect of compositions of the two block copolymers and their length ratio. In order to carry out extensive calculations on the large parameter space, a unit-cell approximation is employed, in which the mean-field equations are solved using a Bessel function expansion. Phase diagrams are constructed for four typical series of blends by comparing the free energies of the different ordered phases including lamellae, cylinders, and spheres. The results reveal that the competition between macro- and microphase separation leads to complex phase behavior. When the length ratio of the two block copolymers is small, the short copolymers tend to segregate to the A/B interfaces, inducing multiple order−order phase transitions including reentrant phase transitions in some blends. When the length ratio of the two diblock copolymers is sufficiently large, macrophase separation may take place. The predicted phase diagrams are compared with available experiments. Density profiles of typical ordered structures are presented to understand the self-organization of the polymer chains. The energetics of the blends is introduced to account for the appearance of the macro- and microphase separations.

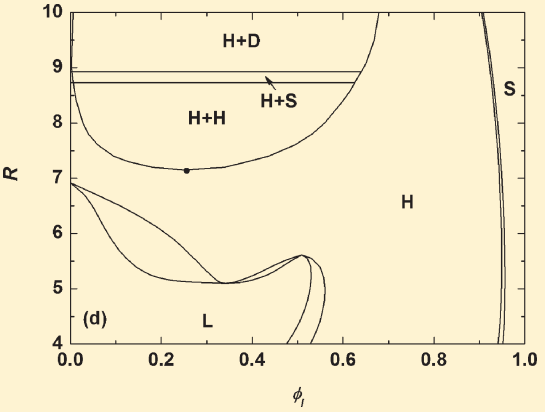

INTRODUCTION

Block copolymers comprising two or more incompatible polymer blocks provide fascinating research topics due to their ability to self-assemble into various ordered structures.[1−3] These structures can be controlled by varying the composition of the block copolymers or the degree of segregation between different blocks. The development of modern synthetic chemistry techniques has made it possible to produce block copolymers with well-defined chain architectures, such as branched and grafted molecules. The chain architecture has been shown to be an additional factor that affects the phase behavior of block copolymers.[4−8] Besides synthesizing new types of copolymers, blending two or more different polymers provides another route to obtain new materials. Especially, blends of two AB-type diblock copolymers have been of considerable experimental[9−24] and theoretical[25−33] interests because this system can be easily modified to yield desired properties in polymeric materials from the same A/B monomers. Several specific topics have been investigated in the studies of these blends, such as the miscibility[10,23,32] and microphase transitions[9,11−13,17−20] as well as the competition between microphase and macrophase transitions.[14−16] These previous investigations show that blends of two AB diblock copolymers exhibit a much complex phase behavior than a neat diblock copolymer. This complexity comes from the competition between macro- and microphase separations as well as the large number of parameters controlling the phase behavior. These parameters include monomer−monomer interactions, chain lengths and compositions of the constituent copolymers, and the blending composition. Despite these previous studies, a comprehensive understanding of the phase behavior of such complex blending systems remains a challenge.

Over the past two decades, sophisticated theories, ranging from analytically approximate descriptions[25−29] to exact numerical methods,[30,34] have been developed to investigate the phase behavior of copolymer blends. Among these theories, the self-consistent field theory[30,34] (SCFT) has proved to be the most powerful one in studying the phase behavior of polymer blends. On the topic of microphase separations, Shi and Noolandi investigated the effects of short chains on the interfacial curvature of structures formed by strongly segregated long chains in binary blends of AB/AB diblock copolymers using SCFT calculations.[30] Their study showed that the addition of a small amount of short chains could lead to appreciable change of the phase diagram.

Received: November 23, 2010
Revised: January 19, 2011
Published: February 09, 2011

The mechanism of the phase transitions mainly depends on the composition of the short diblock copolymers. The short chains behave as compatibilizers concentrated at the domain interfaces when they are symmetric or act more like homopolymer fillers distributed in the majority-block domains when they are asymmetric. The distribution of the short chains determines the stability of the phases with different symmetries. Furthermore, Shi and Noolandi and Matsen have studied the phase behavior of blends composed of two AB diblock copolymers with the same length but different compositions.[31,33] Their results reveal that the phases of these blends can be qualitatively predicted by the one-component approximation if the compositions of the two copolymers are not very different. In the one-component approximation, the phase behavior of the blends is assumed to be governed by two parameters, the incompatibility χN and the total volume fraction of the A monomers in the blends, such that the phase diagram follows that of a neat diblock copolymer. However, if the compositions of the constituent copolymers are rather different, the blends tend to undergo macrophase separation into two disordered phases. On the topic of macrophase separations, Matsen examined binary blends of a long and a short symmetric AB diblock copolymers to investigate the effect of their length ratio on their miscibility using SCFT.[32] He found that the short and the long copolymers are completely miscible if their length ratio is smaller than ~5. As the length ratio exceeds 5, the blend tends to phase separate into two distinct lamellar phases or a lamellar and a disordered phase. Recently, we have examined the phase behavior of blends of a symmetric long and a nearly symmetric short AB diblock copolymers.[35−37] Our studies indicated that the slight asymmetry of the short chains introduces a competition between microphase transition and macrophase transition, and the miscibility criterion is slightly modified from the one for blends composed of two symmetric AB diblock copolymers.[37]

Experimentally, Hashimoto and co-workers have carried out a series of studies on binary blends of polystyrene-*block*-polyisoprene diblock copolymers.[9−20] They systematically studied the phase behavior of these blends and constructed phase diagrams in the parameter space of temperature, blending composition, and molecular weight ratio of the two constituent copolymers. They found that the phase behavior of these blends is much richer than each constituent neat copolymer. A fascinating feature they observed is that stable structures from these blends can break the relationship between morphology and the total composition obtained from a neat diblock copolymer. The one-component approximation works well in predicting the behavior of blends of two diblocks with similar chain length and similar compositions.[31,33] However, as mismatch of the chain lengths or compositions increases, phases beyond those predicted from the one-component approximation may be stabilized. In the experiments, a cylindrical phase was observed in blends of two nearly symmetric diblocks, even when the total volume fraction is close to 0.5.[13−15] Also, a lamellar phase was observed in a blend of an asymmetric long diblock and a symmetric short diblock even when the total volume fraction of the A monomers is close to 0.25.[17] On the theoretical side, a stable cylindrical phase was predicted in blends of two nearly symmetric diblocks, which is in good agreement with the experiment.[28,37] This unexpected phase behavior is due to the intricate competition between interfacial curvature and chain packing.

In the present paper, we report a SCFT study of the phase behavior of blends composed of two AB diblock copolymers with the long one in the strong segregation regime. The effects of compositions of the two constituent diblocks and their length ratio on the stability of various ordered structures and on their miscibility are investigated. Mean-field phase diagrams for four series of blends are constructed by solving the SCFT equations within a unit-cell approximation. A series of ordered structures far beyond those predicted by one-component approximation are found in the phase diagrams. In addition, multiple phase transitions are induced with continuous addition of the short chains. As the length ratio of the two copolymers becomes large, macrophase separation takes place. Density profiles of ordered structures are presented in order to understand the self-organization of the polymer chains.

MODEL AND METHOD

In the present work, numerical SCFT calculations are carried out for an incompressible blend of a long AB diblock copolymer and a short AB diblock copolymer. In the blend, each polymer chain is modeled as a flexible Gaussian chain.[38] The chemical compositions of the two diblock copolymers are characterized by the volume fraction of the A block in each polymer chain, f_{lA} and f_{sA} for the long and the short copolymers, respectively. A parameter, $R = N_l/N_s$, is used to describe the length ratio of the two constituent copolymers, where N_l and N_s are the degrees of polymerization of the long and the short copolymers, respectively. The monomer density ρ_0 and the statistical Kuhn length b are assumed to be the same for the A and B monomers. The interaction between the A and B segments is modeled by a Flory−Huggins interaction parameter χ. The SCFT for a blend can be cast in either the canonical formalism[39] or the grand-canonical approach.[34] Since the two methods are equivalent and the latter is more convenient to discuss the two-phase coexistence regions, the present study is carried out using SCFT in the grand-canonical formalism. The detailed derivation of the grand-canonical SCFT can be found in our previous paper.[37] In general, the SCFT equations cannot be solved analytically. To obtain the mean-field solutions, the equations are usually solved self-consistently using numerical methods. For the ordered structures, Matsen and Schick invented an efficient method which utilizes the symmetry properties of the phase.[40,41] Specifically, these SCFT equations are reformulated in the reciprocal space with a set of basis functions. The basis functions are chosen as the eigenfunctions of the Laplace operator with appropriate boundary conditions consistent with the symmetry of the ordered phase under investigation, where the anisotropic Wigner−Seitz unit cells should be employed. In terms of the expansion coefficients, the SCFT equations become a set of nonlinear algebraic equations which can be solved numerically. In this work, in order to explore much higher degrees of segregation, a unit-cell approximation is employed for the cylindrical and spherical phases, in which the Wigner−Seitz unit cell of these phases are approximated by a circular and a spherical unit cell, respectively. The unit-cell approximation has been demonstrated to be a good approximation in block copolymer blends.[30,31,42] In the present study, the employment of the unit-cell approximation has greatly enhanced the computational efficiency, especially in cases where the short copolymer is very asymmetric. Following the work of Matsen,[42] we choose the Bessel functions as the basis functions. Because of the unit-cell approximation, our work is restricted to the three classical morphologies: lamellae (L), cylinders (H), and spheres (S). This choice of phases excludes the bicontinuous

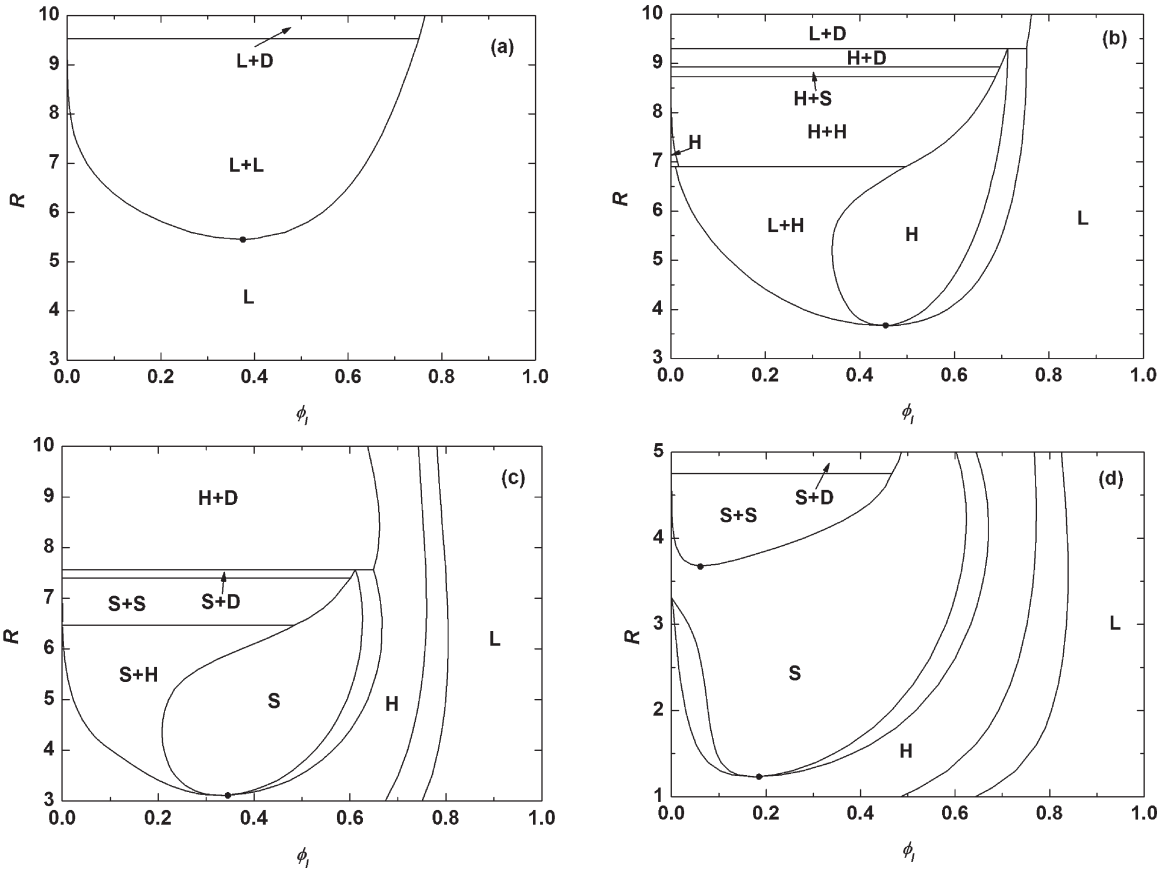

Figure 1. Phase diagrams for binary blends of a long symmetric diblock copolymer and a short diblock copolymer in terms of the concentration of long copolymer ϕ_l and the length ratio R. For all the cases, the degree of segregation is set to be $\chi N_l = 100$. The composition of the short copolymer is (a) $f_{sA} = 0.5$, (b) $f_{sA} = 0.4$, (c) $f_{sA} = 0.3$, and (d) $f_{sA} = 0.2$. The L, H, S, and D represent lamellar, cylindrical, spherical, and disordered phases, respectively.

gyroid phase, which is expected to occur in a small region along the lamellar−cylindrical phase boundary. For an ordered structure, the free energy is minimized with respect to the domain size. Comparing the free energy of different phases allows us to construct the phase diagrams. Furthermore, the free energy calculations provide other relevant quantities such as domain sizes and density profiles. Although the calculations are performed in the grand-canonical ensemble, our results are presented as a function of the average volume concentration of the long diblock copolymer in the blend, $\phi_l = n_l N_l/(n_l N_l + n_s N_s)$, as a variable, where n_l and n_s are the total numbers of the long and the short copolymers, respectively.

RESULTS AND DISCUSSION

Theoretically, in a binary AB/AB diblock copolymer blend, there are five independent controlling parameters, including χN_l, f_{lA}, f_{sA}, ϕ_l, and R. In order to investigate the interplay between the macrophase separation and microphase separation in the strong segregation regime, we fix $\chi N_l = 100$, which is considerably higher than that used in previous SCFT studies.[31,33] Moreover, we focus on the following four series of blends: (i) The long copolymer is symmetric, i.e., $f_{lA} = 0.5$, and the composition of the short copolymer is varied. (ii) The short copolymer is set to be symmetric, $f_{sA} = 0.5$, and the long one is asymmetric. (iii) Both copolymers are asymmetric, and the B block is the majority component in the blends. (iv) Both copolymers are asymmetric but with complementary compositions. For each series of the blends, 1−6 phase diagrams are constructed in terms of ϕ_l and R, where ϕ_l is in the range of 0−1 and R in a wide range. The SCFT equations are solved for the L, H, S, and disordered (D) phases, and the relative stability of these phases is determined by comparing their free energies. For all the ordered structures, up to 120 basis functions are used to ensure that the concentration and field accuracy is smaller than 10^{-6}. Besides phase diagrams, density profiles of different monomers have also been computed.

1. Blends of a Long Symmetric Copolymer and a Short Copolymer. Figure 1 shows the phase diagrams of AB/AB diblock copolymer blends, where the long diblock copolymer is symmetric ($f_{lA} = 0.5$) and the composition of the short one is changed from $f_{sA} = 0.5$ to $f_{sA} = 0.2$. In Each phase diagram, the single-phase regions are labeled and regions of two-phase coexistence are unlabeled, except for some special cases where they are labeled for the convenience of discussion. For all the cases shown in Figure 1, the neat long copolymer shows a well-ordered lamellar phase due to its symmetric composition and relatively strong degree of segregation. The short copolymer is in a disordered state or shows an ordered phase depending on its composition and length. For the case with $f_{sA} = 0.5$, as shown in Figure 1a, the short diblock copolymer shows a lamellar phase when $R < 9.528$, and it is in a disordered state for $R > 9.528$. Obviously, in the whole phase diagram, lamellar phase is the only stable ordered structure due to the symmetry of the system. The critical length ratio is at $R_c \approx 5.45$, below which the two copolymers are completely miscible and form a lamellar structure together. Above this critical value of R, the two copolymers phase

dx.doi.org/10.1021/ma1026687 |*Macromolecules* 2011, 44, 1680–1694

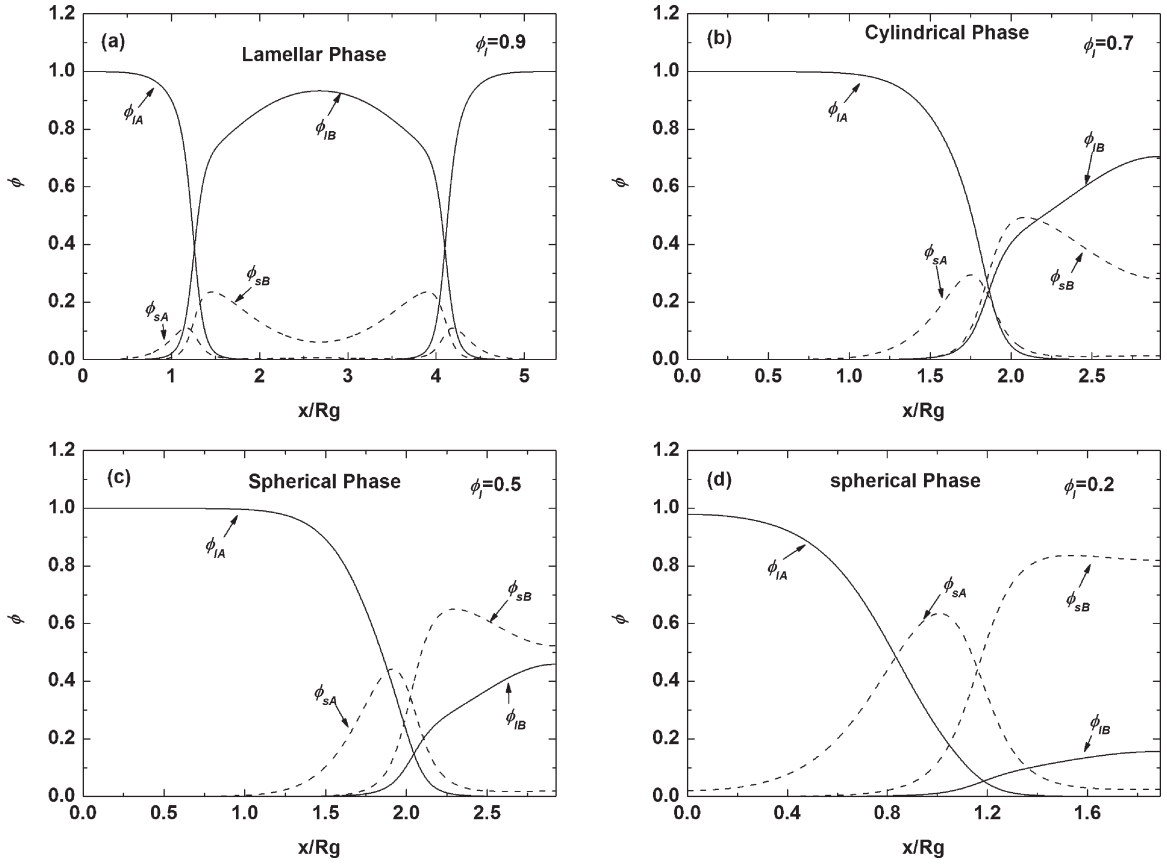

Figure 2. Density profiles for blends with $f_{lA} = 0.5$, $f_{sA} = 0.2$, $\chi N_l = 100$, $R = 3.5$ and (a) $\phi_l = 0.9$, (b) $\phi_l = 0.7$, (c) $\phi_l = 0.5$, and (d) $\phi_l = 0.2$. The corresponding equilibrium ordered structures are labeled in the figure. The profiles of the lamellar structure are plotted over one period, and those of the cylindrical phase and the spherical phase are plotted from the center to the edge of an approximated unit cell along the radial direction. Profiles for the long chains are plotted as solid lines, and those for the short chains are plotted as dashed lines. The length is scaled by the Gaussian radius of gyration of the long diblock copolymer, R_g.

separate into coexistence of two lamellar phases with different periods first and then coexistence of a lamellar phase rich in the long chains and a disordered phase rich in the short chains as their length ratio increases. The result shown in Figure 1a is consistent with that of Matsen on the same kind of blends using SCFT.[32]

Figure 1b gives the phase diagram for the case with $f_{sA} = 0.4$. Although the composition of the short chain is only slightly asymmetric, the topology of the phase diagram deviates considerably from that shown in Figure 1a. The most important feature is the appearance of a cylindrical phase. As shown in Figure 1b, over the range of length ratio, $3.67 < R < 6.9$, both the neat long and short copolymer self-assemble into a lamellar phase by themselves. However, a cylindrical phase can be stabilized over a wide range of ϕ_l. The cylindrical phase can also be found when the neat short copolymer shows a cylindrical phase or a disordered phase as R increases from 6.9 up to 9.3, where the ϕ_l region of the cylindrical phase shrinks quickly with the increase of R. When $R > 9.3$, the cylindrical phase disappears. Another important feature of Figure 1b is a shift of the critical length ratio to $R_c \approx 3.67$. As shown in Figure 1b, when the length ratio $R < 3.67$, the short chains can be added into the blend without producing a macrophase separation, where the two copolymers mix together to form a lamellar phase. When $R > 3.67$, the blend becomes immiscible along with the occurrence of the cylindrical phase, phase separating into coexistence of L + H. Before the macrophase separation, the long diblocks can absorb up to 66% of the short chains in volume. As R increases further, the following coexisting phases appear successively, H + H (the coexistence of two cylindrical phases with different domain sizes), H + S, H + D, and eventually L + D when $R \sim 10$ before the cylindrical phase is stabilized, and the ϕ_l region of these coexisting phases expands rapidly. In these cases, the macrophase separation has suppressed the microphase separation. The phase diagram shown in Figure 1b corresponds well with the one obtained in our previous study.[37] In that work, the phase behavior of the same blends was investigated using SCFT based on real Wigner−Seitz unit cells. This consistency provides an evidence that the unit-cell approximation provides reasonable results. Moreover, the phase diagram agrees well with the one obtained in experiments.[14] The detailed analysis and comparisons with experiments can be found in our previous work.[37]

Figure 1c shows the phase diagram for the case with $f_{sA} = 0.3$, where several new features are found. First, the transition between the lamellar and cylindrical phases always happens, at $\phi_l = 0.7-0.8$, over the whole range of R considered. Second, a spherical phase can be stabilized under certain conditions. Especially, when $3.1 < R < 6.47$, the neat short copolymer shows a cylindrical phase and the long one shows a lamellar phase, but the blend gives a spherical phase over a wide range of ϕ_l. As R increases, the neat short copolymer exhibits a series of phases including a cylindrical, a spherical, and eventually a disordered

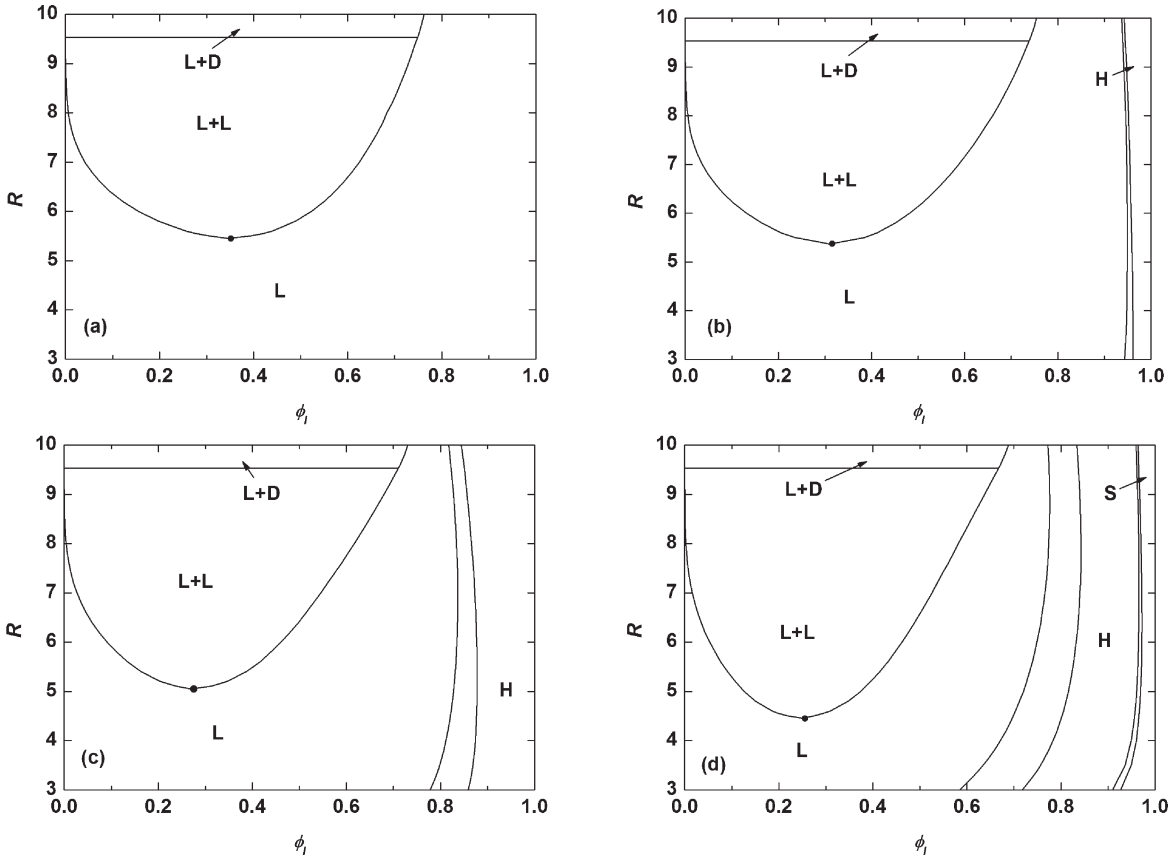

Figure 3. Phase diagrams for binary blends of a long asymmetric diblock copolymer and a short symmetric diblock copolymer in terms of the concentration of the long copolymer ϕ_l and the length ratio R when $\chi N_l = 100$. The composition of the long copolymer is (a) $f_{lA} = 0.4$, (b) $f_{lA} = 0.3$, (c) $f_{lA} = 0.2$, and (d) $f_{lA} = 0.1$.

phase in succession, where the region of the spherical phase expands first, then shrinks, and finally ends at $R \approx 7.57$. Accordingly, starting from $R = 3.1$, the coexisting phases of S + H appears and is followed successively by S + S, S + D, and H + D as R increases. Before the macrophase separation, the long diblock can absorb up to 79% short chains in volume. Comparing with the case shown in Figure 1b, the effect of the short chains on the microphase transition is enhanced in this case, which is attributed to the more asymmetric composition of the short copolymer, and hence the long chains can absorb more short chains before the macrophase separation takes place.

The phase diagram for the case with $f_{sA} = 0.2$ is shown in Figure 1d, where the range of R is $1 \leq R \leq 5$. When $R > 5$, due to the occurrence of a highly swollen spherical phase, it becomes difficult to numerically compute the phase boundaries. As can be seen in Figure 1d, analogous to the case with $f_{sA} = 0.3$, a phase transition from a lamellar to a cylindrical phase always happens. Moreover, with the addition of the short chains, all the classical phases can be obtained in the range of $1.2 < R < 3.7$. Another observation is that, even though the short copolymer is cylinder-forming by itself, a spherical phase can be stabilized over large regions of R and ϕ_l. However, the large region of two-phase coexistence does not appear immediately along with the occurrence of the spherical phase in Figure 1d. In contrast, the macrophase separation appears until the length ratio of the two copolymers increases to $R \approx 3.7$, producing a coexistence of two spherical phases with different domain sizes, and to $R \approx 4.7$, a coexistence of S + D. Over the range of $1.2 < R < 3.7$, the blends are almost miscible. When $R < 1.2$, the length of the short copolymer approaches that of the long one, the spherical phase eventually disappears, and only lamellar and cylindrical phases are stable ordered structures.

The density profiles of ordered structures provide valuable information for the understanding of the self-organization of polymer chains in these structures. For the series of blends of a long symmetric copolymer and a short asymmetric copolymer, the density profiles of typical ordered structures are shown in Figure 2, where the parameters are fixed to be $\chi N_l = 100$, $f_{lA} = 0.5$, $f_{sA} = 0.2$, and $R = 3.5$. As shown in Figure 2, the ordered phases with nonzero interfacial curvature always have an A-rich core since that the A block is the minority component in the blends. For all the cases shown in Figure 2, the long and the short copolymers always share a common interface in order to avoid the contact between unlike monomers. The maximum densities for the A and B monomers of the short chains always appear near the interface, which means that the long chains always stretch further than the short chains. From Figure 2c,d, it is noted that once the spherical phase is stabilized, with the increase of the concentration of the short copolymer, the domain size decreases.

2. Blends of a Long Asymmetric Copolymer and a Short Symmetric Copolymer. The above discussion demonstrates that the addition of the short asymmetric diblock copolymer has a large effect on the stability of the ordered structures formed by the lamella-forming long diblock copolymer, for example, the appearance of cylindrical and spherical phases. Such an effect is enhanced as the degree of asymmetry of the short copolymer

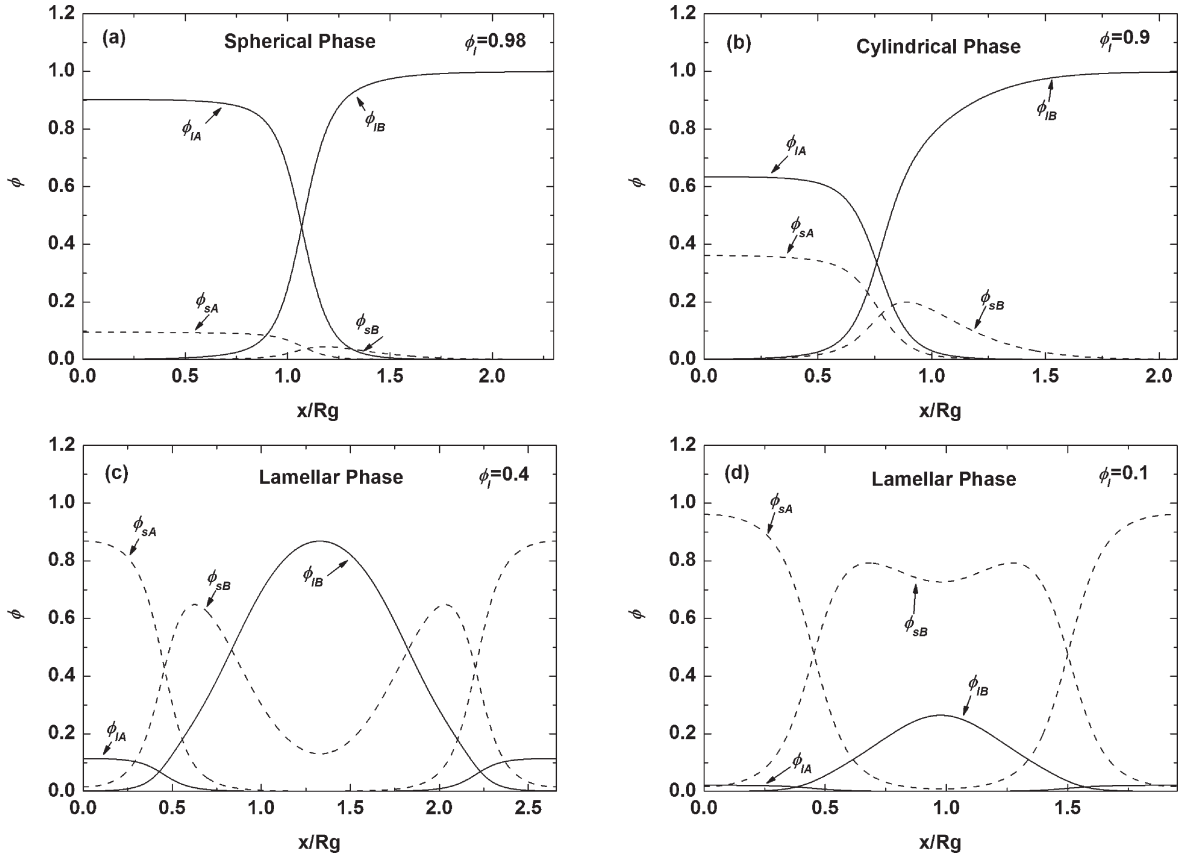

Figure 4. Density profiles for binary blends of a long asymmetric diblock copolymer and a short symmetric diblock copolymer with $\chi N_l = 100$, $f_{lA} = 0.1$, $f_{sA} = 0.5$, $R = 5$, and (a) $\phi_l = 0.98$, (b) $\phi_l = 0.9$, (c) $\phi_l = 0.4$, and (d) $\phi_l = 0.1$. The corresponding equilibrium structures are labeled in the figure. Profile ranges and line type scheme are the same as those in Figure 2.

increases. As a consequence, the miscibility of the blends is also influenced. In this subsection, we focus on binary blends of a long asymmetric diblock copolymer and a short symmetric diblock copolymer. The phase diagrams are shown in Figure 3, where the composition of the short copolymer is fixed at $f_{sA} = 0.5$, and the composition of the short one is changed from $f_{sA} = 0.4$ to $f_{sA} = 0.1$. Before we started, it is useful to describe the equilibrium structures of the neat short and long diblock copolymers. Because of its symmetric composition, the neat short copolymer shows a lamellar phase or a disordered phase. The transition between the ordered and disordered phases for the short diblock copolymers occurs at $R = 9.528$. The long copolymer shows a lamellar phase for $f_{lA} = 0.4$, cylindrical phases for $f_{lA} = 0.3$ and 0.2, and a spherical phase for $f_{lA} = 0.1$. We first focus on the effect of the addition of short chains on the ordered structures formed by the long chains. As we can see in the phase diagram shown in Figure 3a, for the case with $f_{lA} = 0.4$, there is no transitions between ordered phases, which is similar to that shown in Figure 1a. On the other hand, in the cases with $f_{lA} = 0.3$, 0.2, and 0.1, phase transitions occur as shown in Figure 3b−d. Furthermore, independent of the structures formed by the neat long diblock copolymer, the addition of the symmetric short chains always leads to a decrease of the interfacial curvature, eventually stabilizing a lamellar phase. Specifically, for the cases where the neat long copolymer forms cylinders, phase transition from a cylindrical to a lamellar phase is observed (as shown in Figure 3b,c). For the case where the neat long copolymer forms spheres, the addition of short chains induces transitions from a spherical to a cylindrical and finally to a lamellar phase (as shown in Figure 3d). One fascinating feature is that phase transitions from a cylindrical to a lamellar phase or from a spherical to a cylindrical phase can happen when only a small amount of (∼5%) short chains are added, as shown in Figure 3b,d. Another fascinating feature is that for some lamellar structures found in Figure 3c, d the total volume fraction of the blend is less than 0.3. For example, in Figure 3d, at the point $\phi_l = 0.7$ and $R = 7$, a lamellar structure is found. Corresponding to that point, the total volume fraction of A monomers in the blend is only $f_{lA}\phi_l + f_{sA}(1 - \phi_l) = 0.22$. On the other hand, with such a small volume fraction, only cylindrical or spherical phases can be expected in a neat diblock copolymer. This result indicates that the stability mechanism of an ordered structure in these binary blends is quite different from that in the neat diblock copolymers. As for the miscibility, in all the cases shown in Figure 3, after the lamellar phase is stabilized and above a critical point, a further increase of the amount of short chains leads to a macrophase separation, producing coexistence of two lamellar phases with different periods or coexistence of a lamellar phase rich in the long copolymer and a disordered phase with mostly of the short copolymer. This feature is similar to that observed in the blend of two symmetric copolymers as shown in Figure 1a. Combining Figure 3 and Figure 1a, the following conclusions can be drawn from the five phase diagrams with $f_{sA} = 0.5$: the more symmetric the long copolymer is, more short chains can be absorbed before the macrophase separation, and the critical length ratio is higher. In their experiments,[17] Hashimoto and co-workers studied the phase behavior

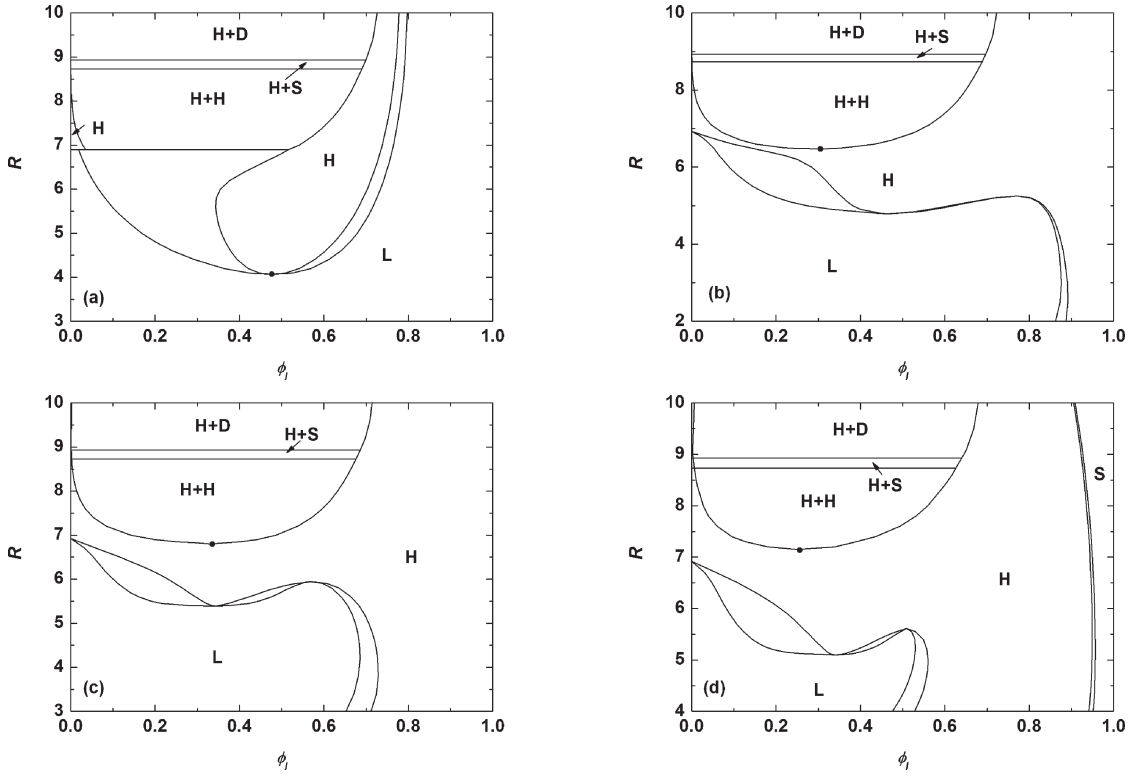

Figure 5. Phase diagrams for binary blends of two asymmetric diblock copolymers in terms of the concentration of long copolymer ϕ_l and the length ratio R with $\chi N_l = 100$. The composition of the short chains is set to be $f_{sA} = 0.4$, and the composition of the long chain is (a) $f_{lA} = 0.4$, (b) $f_{lA} = 0.3$, (c) $f_{lA} = 0.2$, and (d) $f_{lA} = 0.1$.

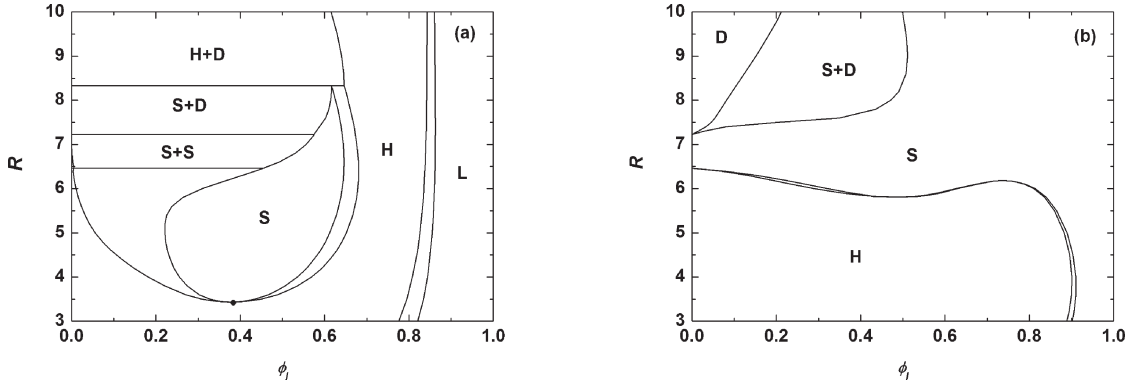

Figure 6. Phase diagrams for binary blends of two asymmetric diblock copolymers in terms of the concentration of long copolymer ϕ_l and the length ratio R when $\chi N_l = 100$. The composition of the short chains is set to be $f_{sA} = 0.3$, and the composition of the long chain is (a) $f_{lA} = 0.4$ and (b) $f_{lA} = 0.1$.

of binary AB diblock copolymer blends composed of a long sphere-forming copolymer and a short symmetric copolymer. The blends are investigated at ambient temperature (relatively strong segregation). The length ratio they considered is in the range of $2.9 < R < 4.4$. They observed that over the whole composition range the blends do not undergo macrophase separation but self-organize into either a single ordered phase or a single disordered phase. The ordered phases they observed are classical phases of the neat AB diblock copolymer and in the order from lamellae to bicontinuous, to cylinders, and finally to spheres with decreasing the total volume fraction of A monomers in the blends. Their experimental condition is similar to the case shown in Figure 3d. Considering that the total volume fraction of the A monomers increases monotonously as the concentration of the short chains increases, most of their observed phase transitions agree with our theoretical predictions, except for the bicontinuous phase which is not included in the current calculations. In addition, a lamellar phase was found in their experiments even if the total volume fraction is 0.25, which also agrees with our predictions. However, there are differences between their experiments and our predictions. The most important one is that macrophase separation was not found in their experiment. This may be attributed to the following possible reasons. First, the degree of segregation is not strong enough in their samples, which prevented the occurrence of macrophase separation. Second, the value of R considered in their experiment is relatively small, macrophase did not occur, or even if it had occurred in a narrow region of the blending composition, it was difficult to be observed.

dx.doi.org/10.1021/ma1026687 |*Macromolecules* 2011, 44, 1680–1694

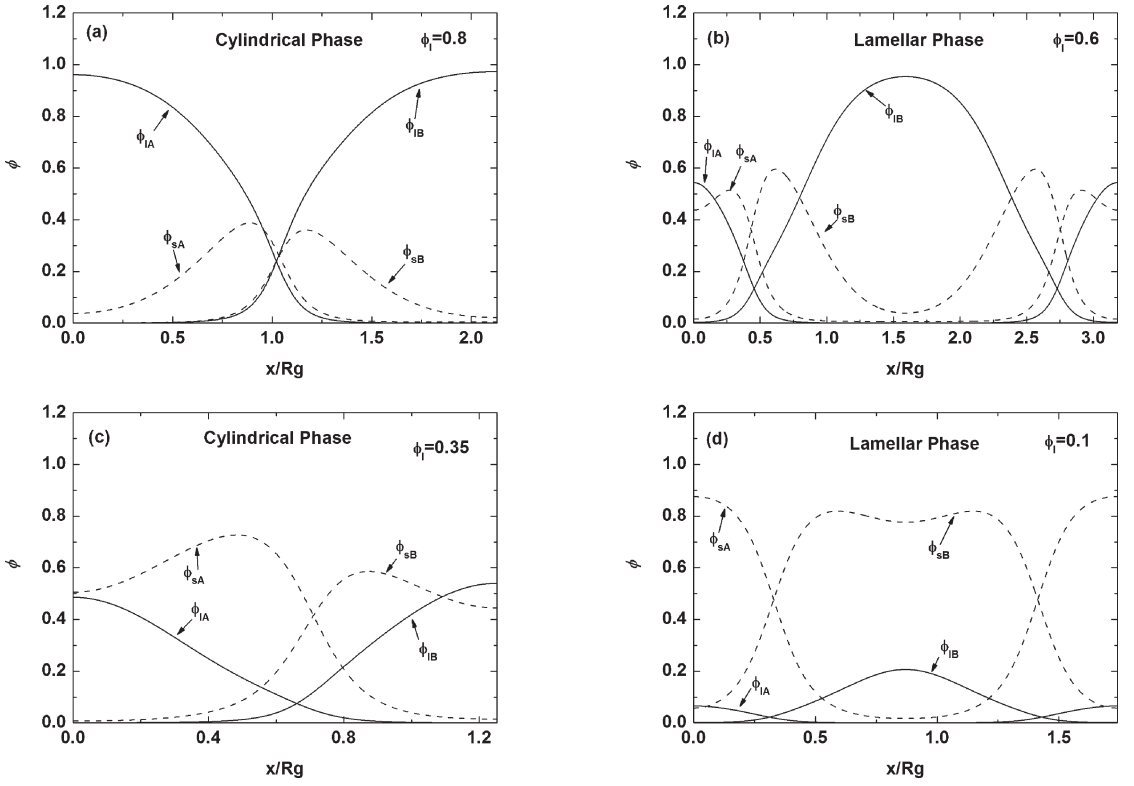

Figure 7. Density profiles for blends of two asymmetric diblock copolymers with $\chi N_l = 100$, $f_{lA} = 0.2$, $f_{sA} = 0.4$, $R = 5.75$, and (a) $\phi_l = 0.8$, (b) $\phi_l = 0.6$, (c) $\phi_l = 0.35$, and (d) $\phi_l = 0.1$. The corresponding equilibrium structures are labeled in the figure. Profile ranges and line type scheme are the same as those in Figure 2.

For blends of a long asymmetric copolymer and a short symmetric copolymer, density profiles of typical ordered structures are shown in Figure 4. The parameters are fixed to be $\chi N_l = 100$, $f_{lA} = 0.1$, $f_{sA} = 0.5$, and $R = 5$. It is noted that in all the profiles the short and the long copolymers share a common interface. In Figure 4a,b, the asymmetric density distribution of the A and B monomers for the symmetric short copolymer arises from the interfacial curvature of the sphere and cylinder, respectively. As sufficient short chains are added, a lamellar phase is stabilized. Parts c and d of Figure 4 show the density profiles for the lamellar structures formed when $\phi_l = 0.4$ and 0.1, respectively. It is observed that as the concentration of the short chains increases, the domain size of the lamellar phase decreases, which accords with previous experiments.[18]

3. Blends of Two Asymmetric Copolymers with B Block as the Majority Component. As shown in the above discussion, the addition of asymmetric short chains tends to increase the interfacial curvature of a lamellar phase formed by the long symmetric copolymer, whereas the addition of symmetric short chains tends to decrease the interfacial curvature of a cylindrical or a spherical phase formed by the long asymmetric copolymer. However, as shown in the following discussion, a slightly asymmetric short copolymer can both increase and decrease the interfacial curvature even in one type of blend. Figure 5 shows the phase diagrams for the blends of two asymmetric diblock copolymers. The composition of the short copolymer is fixed as $f_{sA} = 0.4$, and that of the long copolymer changes from $f_{lA} = 0.4$ to $f_{lA} = 0.1$ so that in all the blends the B block is the majority component. As shown in Figure 5a for the case with $f_{lA} = 0.4$, the neat long copolymer forms a lamellar phase, and the addition of

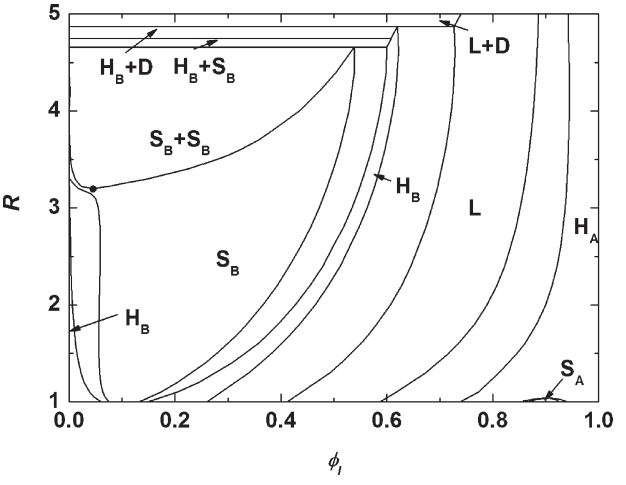

Figure 8. Phase diagrams for binary blends of two asymmetric diblock copolymers in terms of the concentration of long diblocks ϕ_l and the length ratio R when $\chi N_l = 100$. The compositions of the two copolymers satisfy $f_{lA} = 1 - f_{sA} = 0.2$. For clarity, the A-rich and B-rich phases have been designated with subscript labeled in the H and S in the figure.

the short chains tends to increase the interfacial curvature of the lamellar phase. In this case, the phase diagram is very similar to that in the case with $f_{lA} = 0.5$ and $f_{sA} = 0.4$, except the differences that up to $R = 10$ the cylindrical phase is still stable, and the phase transition from lamellar to cylindrical phases needs less short chains in the former case compared with that in the latter case. These differences demonstrate that in the case with $f_{lA} = 0.4$ the

dx.doi.org/10.1021/ma1026687 |*Macromolecules* 2011, 44, 1680–1694

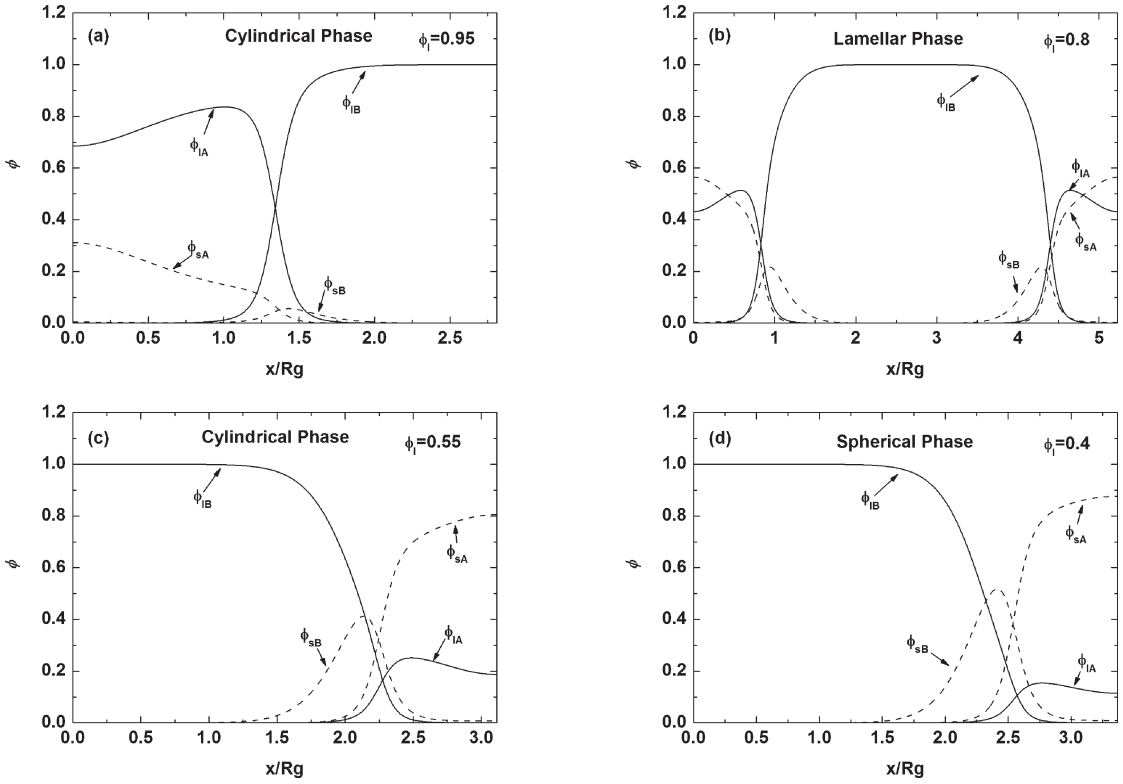

Figure 9. Density profiles for blends of two asymmetric diblock copolymers with $\chi N_l = 100$, $f_{lA} = 0.2$, $f_{sA} = 0.8$, $R = 3.0$, and (a) $\phi_l = 0.95$, (b) $\phi_l = 0.8$, (c) $\phi_l = 0.55$, and (d) $\phi_l = 0.4$. The corresponding equilibrium ordered structures are labeled in the figure. Profile ranges and line type scheme are the same as those in Figure 2.

interfacial curvature is much easily to be bended than that in the case with $f_{lA} = 0.5$ as the short chains are added. On the other hand, in the case with $f_{lA} = 0.3$ and $f_{sA} = 0.4$ where the long copolymer is cylinder-forming by itself, as shown in Figure 5b, a phase transition from a cylindrical phase to a lamellar phase happens as a small amount of (∼10%−20%) the short chains is blended in the range of $2 < R < 5.25$. The transition means that the short copolymer provides an effect of decreasing the interfacial curvature of the ordered structures formed by the long copolymer. However, surprisingly, in the range of $4.79 < R < 5.25$, with a further continuous addition of the short chains, phase transitions from the lamellar phase to the cylindrical phase and then from the cylindrical phase to the lamellar phase happen in succession. This series of reentrant phase transitions may be due to the competition between the two effects of the short chains on the interfacial curvature. Similar results can be found in the case with $f_{lA} = 0.2$, in the range of $5.39 < R < 5.94$, as shown in Figure 5c. And in Figure 5d for the case with $f_{lA} = 0.1$, as the short chains are added, a phase transition from a spherical phase to a cylindrical phase takes place first, and then a series of phase transitions, from cylindrical to lamellar, from lamellar to cylindrical, and then from cylindrical to lamellar, happen in the range of $5.1 < R < 5.61$, similar to those observed in Figure 5b,c. Besides order−order phase transitions, macrophase separations can also be found in Figure 5b−d. When the length ratio is sufficiently large, two-phase coexistence of H + H occurs first, and it is replaced by H + S and then by H + D as R increases. An interesting feature found in Figure 5b−d is that each phase diagram can be simply separated into a microphase part and a macrophase part.

Figure 6 shows the phase diagrams for blends with $f_{sA} = 0.3$ and $f_{lA} = 0.4$ and 0.1, where a trend similar to that observed in Figure 5 can be found. In Figure 6a for the case with $f_{lA} = 0.4$, the short chains tend to increase the interfacial curvature, whereas in Figure 6b for the case with $f_{lA} = 0.1$, the short chains tend to decrease the interfacial curvature first and then has a chance to increase it. In Figure 6b, an important feature is that the blends are much miscible, and only a small coexisting region of S + D can be found when $R > 7.23$. This trend is reasonable considering that as the volume fractions of the B monomers in the two constituent copolymers increase, behavior of the binary AB copolymer blends should be gradually approach to that of blends of two B-homopolymers with different lengths; in the latter case, the two polymers are completely miscible.

For blends of two asymmetric diblock copolymers, density profiles of typical ordered structures are shown in Figure 7. The parameters are fixed to be $\chi N_l = 100$, $f_{lA} = 0.2$, $f_{sA} = 0.4$, and $R = 5.75$. For this set of parameters, as the concentration of the short copolymer increases, ordered structures from a cylindrical to a lamellar, to another cylindrical, and finally to another lamellar phase can be obtained. Still, the short and the long chains share a common interface, and with increasing the concentration of the short chains, the domain size of ordered structures shrinks markedly.

4. Blends of Two Asymmetric Copolymers with Complementary Compositions. In this series of blends, we choose the compositions of the two constituent diblock copolymers satisfying $f_{lA} = 1 - f_{sA} = 0.2$; hence, the neat long copolymer is cylinder-forming by itself. The phase diagram of this series of blends is shown in Figure 8, where the value of R considered is in the range of $1 < R < 5$. For the special case with $R = 1$, the phases boundaries should be symmetric with respect to $\phi_l = 0.5$ due to the symmetry of the two constituent copolymers. In Figure 8, it is noted that for

this special case the mainly ordered structures are lamellar and cylindrical phases. However, spherical phases can also be found in small ranges of ϕ_l, around $\phi_l \approx 0.1$ and $\phi_l \approx 0.9$. Phases with similar orders to this special case were observed by Masten in similar blends but in the relatively weak segregation regime over the range $28 < \chi N < 30$.[33] As R increases, the spherical phase around $\phi_l \approx 0.9$ disappears at $R \approx 1.04$. Above that point, over a large range of R, order−order phase transitions from a cylindrical phase with A-rich core to a lamellar phase, to a cylindrical phase with B-rich core, to a spherical phase with B-rich core, and finally to a cylindrical phase with B-rich core take place in succession with the gradual addition of the short chains. This fascinating series of transitions shows that the short chains can bend the interface from the one toward the A monomers to the one toward the B monomers. Such an effect of the short chains is enhanced by the increase of R, where less short chains are needed to cause an order−order phase transition. As a consequence, a series of spherical phases with a total volume fraction of the A monomers close to 0.5 are stabilized. As noted in Figure 8, when we fix the parameters at $R = 4$ and $\phi_l = 0.5$, a spherical phase is found stable; the total volume fraction of the A monomers in the corresponding blend is $f_{lA}\phi_l + f_{sA}(1 - \phi_l) = 0.5$. On the other hand, with such a volume fraction, only a lamellar phase can be expected in the neat diblock copolymer melts. This fact further reveals that the short chains have a large effect on the interfacial curvature. On the macrophase separation side, coexistence of two spherical phases with different domain sizes appears when $R > 3.2$, and two-phase coexistences of $H_B + S_B$, $H_B + D$, and $L + D$ appear in succession with the gradual increase of R. The ϕ_l region of these coexistences expands with the increase of R, which causes the disappearance of the S_B at $R \approx 4.66$ and then of the H_B at $R \approx 4.87$. Using an analytic theory in the strong segregation limit, Birshtein et al. provided a theoretical study on a binary blend of two asymmetric diblock copolymers. In their study, one copolymer is A-rich and forms a cylindrical phase by itself, whereas another one is B-rich and forms an inverse cylindrical phase by itself, and the A blocks of the two copolymers have the same length.[29] According to their results, phase transition from a cylindrical to a lamellar phase always took place as the amount of the short chains increases, which agrees well with our results. However, the spherical phase was not considered in their work; therefore, the coexistence was predicted as that of two cylindrical phases, which disagrees with our results. On the other hand, a double-cylindrical phase was also found in their phase diagram.

For the series of blends of two asymmetric copolymers with complementary compositions, the density profiles of typical ordered structures are shown in Figure 9. The parameters are fixed to be $\chi N_l = 100$, $f_{lA} = 0.2$, $f_{sA} = 0.8$, and $R = 3.0$. Figure 9a shows the density profiles for the case when a small amount (5%) of the short chains are added, where the cylindrical structure formed by the neat long copolymer remains. In this case, the two kinds of chains share a common interface. In addition, a large part of the A monomers from the short copolymer distribute into the A-rich core due to their relatively larger length than those of the long chains, which helps to flat the domain interface and hence causes the phase transition from the cylindrical phase to a lamellar phase. Figure 9b shows the density profiles for the case when 20% of the short chains are added, where a lamellar phase is stabilized. In this case, the A blocks of the short chains stretch further than those of the long chains because of their relative larger length. Parts c and d of Figure 9 show the density profiles for the cylindrical phase and the spherical phase with B-rich cores, respectively. In these cases, more A monomers of the short chains are filled into the A-rich domain.

5. Energetics of Phase Separations. In order to understand the macro- and microphase separations, we discuss the energetics of the blends. To be specific, we discuss the problem in the canonical ensemble. According to SCFT, the free energy density of the blend is[30]

$$\frac{NF}{k_B T \rho_0 V} = \frac{1}{V}\int \mathrm{d}r[\chi N \phi_A(\mathbf{r})\phi_B(\mathbf{r}) - \omega_A(\mathbf{r})\phi_A(\mathbf{r}) - \omega_B(\mathbf{r})\phi_B(\mathbf{r})] - \phi_l \ln Q_l - R(1-\phi_l)\ln Q_s + f_{mix} \quad (1)$$

where Q_l and Q_s are the single-chain partition functions of the long and the short copolymers, respectively, ϕ_A and ϕ_B are the monomer densities, and ω_A and ω_B are the corresponding conjugate fields for monomers A and B.

The Helmholtz free energy can be decomposed into the following components

$$F = U - T(S_{lJ} + S_{sJ} + S_{lA} + S_{lA} + S_{sA} + S_{sB} + S_{mix}) \quad (2)$$

where U is defined as the internal energy arising from the interaction between A and B monomers. S_{lJ} and S_{sJ} are the translational entropy of junctions of the long and the short copolymer chains, respectively. S_{lA}, S_{lB}, S_{sA}, and S_{sB} are the configurational entropies of the A and B blocks of the long and the short chains, respectively, and S_{mix} is the mixing entropy for a homogeneous phase. Accordingly, the free energy density f can be expressed as

$$f = \frac{NF}{k_B T \rho_0 V} = f_{in} + f_{lJ} + f_{sJ} + f_{lA} + f_{lB} + f_{sA} + f_{sB} + f_{mix} \quad (3)$$

Following the strategy proposed by Matsen and Bates,[43] the different terms in the right side of eq 3 can be written as

$$f_{in} = \frac{NU}{k_B T \rho_0 V} = \frac{\chi N}{V}\int \mathrm{d}r\, \phi_A(\mathbf{r})\phi_B(\mathbf{r}) \quad (4)$$

$$f_{lJ} = -\frac{NS_{lJ}}{k_B \rho_0 V} = \frac{\phi_l}{V}\int \mathrm{d}r\, \rho_l(\mathbf{r}) \ln \rho_l(\mathbf{r}) \quad (5)$$

$$f_{sJ} = -\frac{NS_{sJ}}{k_B \rho_0 V} = \frac{R(1-\phi_l)}{V}\int \mathrm{d}\mathbf{r}\, \rho_s(\mathbf{r}) \ln \rho_s(\mathbf{r}) \quad (6)$$

$$f_{lA} = -\frac{NS_{lA}}{k_B \rho_0 V} = -\frac{\phi_l}{V}\int \mathrm{d}\mathbf{r}\, [\rho_{lJ}(\mathbf{r}) \ln q_{lA}(\mathbf{r}, f_{lA}) + \omega_A(\mathbf{r})\phi_{lA}(\mathbf{r})] \quad (7)$$

$$f_{lB} = -\frac{NS_{lB}}{k_B \rho_0 V} = -\frac{\phi_l}{V}\int \mathrm{d}\mathbf{r}\, [\rho_{lJ}(\mathbf{r}) \ln q_{lB}(\mathbf{r}, f_{lB}) + \omega_B(\mathbf{r})\phi_{lB}(\mathbf{r})] \quad (8)$$

$$f_{sA} = -\frac{NS_{sA}}{k_B \rho_0 V} = -\frac{R(1-\phi_l)}{V}\int \mathrm{d}\mathbf{r}\, [\rho_{sJ}(\mathbf{r}) \ln q_{sA}(\mathbf{r}, f_{sA}/R) + \omega_A(\mathbf{r})\phi_{sA}(\mathbf{r})] \quad (9)$$

$$f_{sB} = -\frac{NS_{sB}}{k_B \rho_0 V} = -\frac{R(1-\phi_l)}{V}\int \mathrm{d}\mathbf{r}\, [\rho_{sJ}(\mathbf{r}) \ln q_{sB}(\mathbf{r}, (1-f_{sA})/R) + \omega_B(\mathbf{r})\phi_{sB}(\mathbf{r})] \quad (10)$$

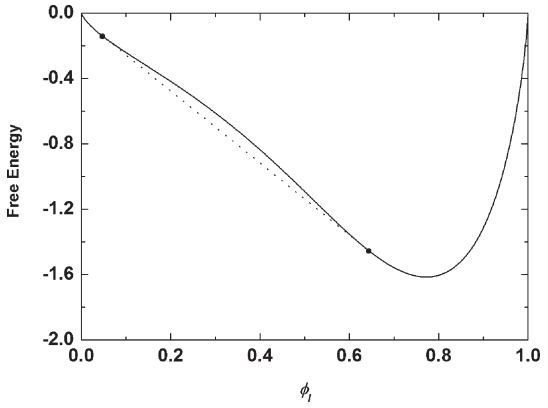

Figure 10. Helmholtz free energy (for clarity, we add $c_1\phi_l + c_0$ to the free energy to shift the free energy curve satisfies that $f(0) = f(1) = 0$, which does not affect the analysis). The parameters are $\chi N = 100$, $f_{lA} = f_{sA} = 0.5$, and $R = 7$. The solid line is the free energy curve, and the dotted line is the common tangent.

$$f_{mix} = -\frac{NS_{mix}}{k_B\rho_0 V} = \phi_l \ln \phi_l + R(1-\phi_l)\ln(1-\phi_l) = f_{mix} \quad (11)$$

where ρ_l and ρ_s are the junction distribution functions of the two chains, and $q_{p\alpha}$ (p = l, s; α = A, B) are the end-integrated propagators, which satisfy the following modified diffusion equation with the initial condition $q_{p\alpha}(\mathbf{r},0) = 1$.

$$\frac{\partial q_{p\alpha}(\mathbf{r}, s)}{\partial s} = \nabla^2 q_{p\alpha}(\mathbf{r}, s) - \omega_\alpha(\mathbf{r}) q_{p\alpha}(\mathbf{r}, s) \quad (12)$$

We take the set of parameters with $\chi N = 100$, $f_{lA} = f_{sA} = 0.5$, and $R = 7$ as an example for the case of macrophase separations. For this particular set of parameters, the two copolymers are both symmetric; hence, the configurational entropies of the blocks satisfy that $S_{lA} = S_{lB}$, $S_{sA} = S_{sB}$. The corresponding Helmholtz free energy for the lamellar phase as a function of blending composition is shown in Figure 10. The dotted line connecting the two blending compositions is the common tangent line, and it is also the free energy of demixed state. From Figure 10, it is noted that in the blending composition interval between $\phi_l = 0.638$ and $\phi_l = 0.042$, to obtain the lowest free energy, the blends phase separate into two lamellar phases with different periods. It is also noted in that blending compositions interval the two lamellar phases resulted from the macrophase separation are never formed by the neat long or short chains alone. They are both mixed phases of the long and the short chains. The long-period lamellar phase contains 36.2% of the short chains, and the short-period lamellar phase contains only about 0.42% of the long chains. Figure 11 shows the components of the Helmholtz free energy for the lamellar phase with the above set of parameters as a function of blending composition. The dotted lines are the corresponding free energy curves of the demixed state when the macrophase separation happens. It is noted that the phase behavior of the blend is determined by the competition among the different components of the free energy. In Figure 11, in the above-mentioned blending composition interval, items f_{mix}, f_{in}, and f_{lJ} (Figure 11, a, b, and c) prefer a mixed single lamellar phase. On the other hand, items f_{sJ}, f_{lA} (f_{lB}), and f_{sA} (f_{sB}) (Figure 11, d, e, and f) prefer a demixed state. That is, when the two copolymers are mixed together sharing a common interface, the free energies from the translational entropy of the short chain (Figure 11d) and from the configurational entropies (Figure 11e,f) of both chains are higher when compared with those in the demixed state. Therefore, decreasing f_{sJ}, f_{lA} (f_{lB}), and f_{sA} (f_{sB}) are the driving forces for the occurrence of the macrophase separation. We may understand the above result based on the following analysis. Among the components of the free energy, the term f_{mix} always prefers a mixed single phase to achieve the maximum mixing entropy. As for the term f_{in}, by sharing a common interface, the copolymers act as surfactant and hence can partly screen the unfavorable contact between the A and B monomers, so f_{in} also prefers a mixed single phase. As for the term f_{lJ}, the interfacial widths of the two lamellae may compromise to an intermediate value by blending the two copolymers, which causes the junctions of the long chains somewhat less confined when compared with that in the lamellae composed mainly of the long chains. So, f_{lJ} also prefers a mixed single phase. On the other hand, the compromised interfacial widths of the two lamellae may cause the junctions of the short chains more confined when compared with that in the lamellae composed mainly of the short chains. Hence, the translational entropy of the short chains decreases, and the corresponding energy increases in a mixed single phase. So, f_{sJ} prefers demixed phases. As for the term f_{lA}, the location of the short chains at the interfaces causes that the long chains near the interfaces are more stretching. Moreover, due to the shrinking of the domain size of the lamellar phase with the addition of the short chains, the long chains tend to be far from the interface to become more relaxed. The combination of the two effects results in an increase in the free energy of the long chain configurational entropy. So, f_{lA} also prefers demixed phases. As for the term f_{sA}, there is a penalty in the energy related to the configurational entropy of the short chain when mixed with the long chains. So, it also prefers demixed phases.

Figure 12 shows the periods of lamellar phase, computed based on the assumption that the blends are miscible and form a single lamellar phase. It is noted that when the short copolymer is the major component in the blend, the periods of the lamellar phase are smaller than $2R_g$ of the long chain for cases with $R = 5$, 6, and 7. In these cases, the periods are too small for the long chains to relax. Therefore, the system prefers to macrophase separate into two phases rather than a mixed phase, and therefore the short chains can absorb few of the long ones.

The phase transitions between the ordered structures can also be understood by comparing each component of the free energy. We take a set of parameters of $\chi N_l = 100$, $f_{lA} = 0.1$, $f_{sA} = 0.5$, and $R = 5$ as an example. From the phase diagram shown in Figure 3d, we note that for blends with this set of parameters phase transitions from spherical to cylindrical and finally to lamellar phase occur with the decrease of the concentration of the long chains in the blend. Figure 13 shows the internal free energy density f_{in} of the blend as a function of blending composition. It is noted that the energy curve exist discontinuous points which correspond to the phase transitions shown in Figure 3d. From Figure 13, we observe that the occurrence of the phase transitions is in favor of decreasing the interaction between unlike monomers.

The other components of the free energy are shown in Figure 14. It is noted that when the phase transitions happen, the components related to the transitional entropies of the two copolymers (f_{lJ} and f_{sJ}) change slightly. However, the energies related to the configurational entropies of the long and the short chains change significantly. At each phase transition point with the addition of the short chains, f_{lA} and f_{sA} decrease, while f_{lB} and f_{sB} increase. That is, as the interfacial curvature decreases, the A

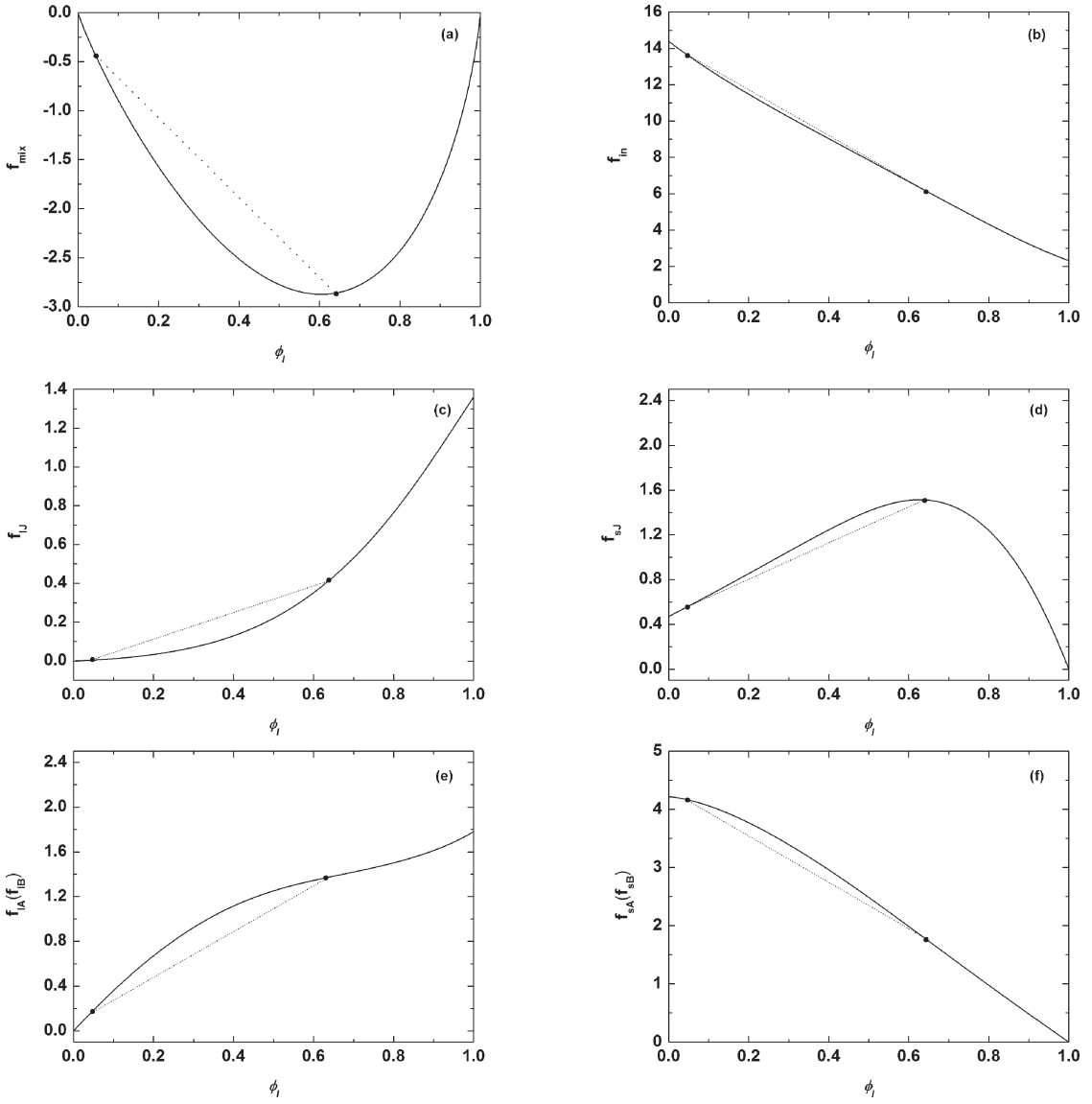

Figure 11. Components of the free energy for the lamellar phase with parameters $\chi N = 100$, $f_{IA} = f_{sA} = 0.5$, and $R = 7$ as a function of blending composition: (a) f_{mix}, (b) f_{in}, (c) f_{IJ}, (d) f_{sJ}, (e) f_{IA} (f_{IB}), and (f) f_{sA} (f_{sB}).

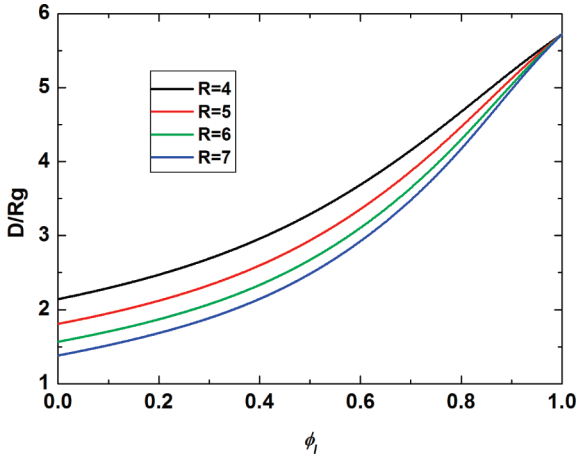

Figure 12. Periods of the lamellar phases as a function of blending composition. They are calculated based on the assumption that the two diblock copolymers are mixed together to form a single phase.

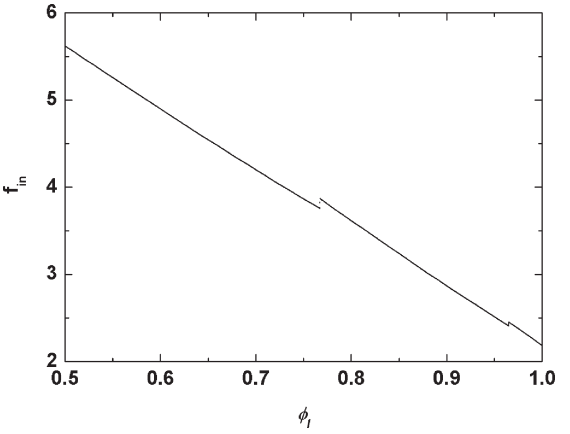

Figure 13. Internal free energy density f_{in} of the blend with parameters $\chi N_I = 100$, $f_{IA} = 0.1$, $f_{sA} = 0.5$, and $R = 5$ as a function of blending composition.

dx.doi.org/10.1021/ma1026687 |*Macromolecules* 2011, 44, 1680–1694

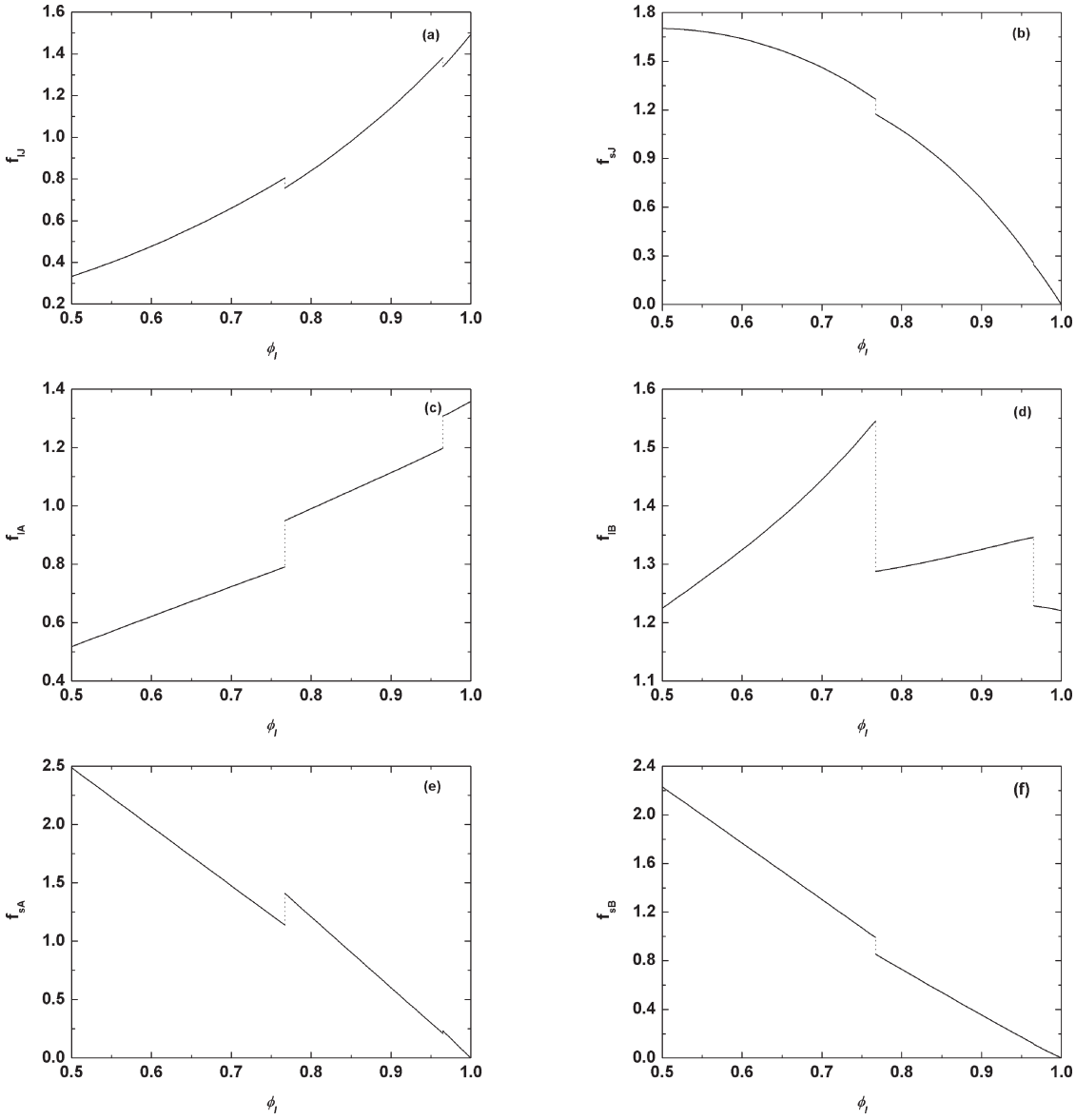

Figure 14. Components of the free energy for blend with parameters $\chi N_l = 100$, $f_{lA} = 0.1$, $f_{sA} = 0.5$, and $R = 5$: (a) f_{lJ}, (b) f_{sJ}, (c) f_{lA}, (d) f_{lB}, (e) f_{sA}, and (f) f_{sB}.

blocks of the two copolymers relax whereas the B blocks stretch, which is consistent with the fact in the neat diblock copolymer melts.[43] Therefore, the phase transitions in the blend are mainly determined by the competition of the interaction between A and B monomers and the configurational entropies. The gain in f_{in} and relaxation of the A blocks of the two copolymers eventually induce the series of phase transitions.

For all the blends considered in the present paper, their macro- and microphase separations may be discussed based on a similar energetic analysis as those listed in the above examples. Their phase behavior must be determined by the competition among the different components of the free energy.

CONCLUSIONS

Phase behavior of blends of two AB diblock copolymers, with the long one at relatively strong segregation regime, is studied using self-consistent field theory within a unit-cell approximation. The influences of compositions of the two constituent copolymers and their length ratio on the stability of ordered structures and on their miscibility are extensively investigated. Studies reveal that the interplay between possible macrophase and microphase separations results in complex phase behavior. Various ordered structures may be stabilized by tuning the blending composition. In the ordered structures, the two constituent copolymers tend to share a common interface, and the concentration of the short chains largely affects the relative stability of ordered structures. Furthermore, due to the mismatch of the chain lengths of the two constituent copolymers, the behavior of microphase separation may not be controlled by the one-component approximation. A series of ordered structures far beyond those predicted from the one-component approximation are found in the phase diagrams. For example, a cylindrical phase is found stable by blending two lamella-forming copolymers, and a spherical phase is found stable by blending a lamella-forming copolymer and a cylinder-forming copolymer. Moreover, a spherical phase is found stable even if the total volume fraction

of the A monomers in the blend is close to 0.5 when the two constituent copolymers are asymmetric and with complementary compositions, and a lamellar phase is found stable even if the total volume fraction of A monomers is less than 0.3 in blends of an asymmetric long copolymer and a symmetric short copolymer. This fascinating feature is due to the enhancement of the effect of the short chains on the interfacial curvatures when the length ratio of the two constituent copolymers increases. Another fascinating feature is that multiple phase transitions can usually be observed with continuous addition of the short chains in a blend, and sometimes a transition happens when only a small amount of the short chains is added. These results indicate that the short chains may change the interfacial curvature of a structure formed by the long copolymer or by the blend. Generally, when blending with a symmetric long copolymer, an asymmetric short copolymer tends to increase the interfacial curvature, whereas when blending with an asymmetric long copolymer, a symmetric short copolymer tends to decrease the interfacial curvature. However, reentrant phase transitions are observed in blends composed of an asymmetric long copolymer and a slightly asymmetric short copolymer, indicating that a slightly asymmetric short copolymer can both increase and decrease the interfacial curvature even in one type of blend. On the other hand, when the length ratio of the two constituent copolymers is sufficient large, macrophase separation may take place, which prevents ordered structures from being stable. In all the phase diagrams we constructed, macrophase separations always happen. And in general, before the macrophase separation, the long copolymer can absorb a considerable amount of short chains, but the short copolymer can absorb a little amount of the long chains. The macro- and microphase separations are discussed based on energetic analysis.

Naturally, our mean-field predictions will be modified somewhat by fluctuations. However, the fluctuation effect should be negligible since that the SCFT calculations performed here are at a relatively strong segregation of the long copolymer. In addition, due to the employment of the unit-cell approximation, ordered phases examined in the calculations are restricted to the classical ones. On the other hand, complicated structures beyond the classical phases, such as the gyroid phase and a distorted bicontinuous structure, were also observed in previous experiments.[17,19,20] However, for studies performed in this work, there is no serious drawback. The gyroid phase generally exists in narrow channel between lamellar and cylindrical phases. Therefore, the region of gyroid phase can be easily suggested in the phase diagrams. The distorted bicontinuous phase was always found at high temperatures (low χN value) in experiments, whereas at relatively strong segregation, it is seldom found.

AUTHOR INFORMATION

Corresponding Author

*E-mail: baohui@nankai.edu.cn (B.L.); shi@mcmaster.ca (A.-C.S.).

ACKNOWLEDGMENT

This research is supported by the National Natural Science Foundation of China (No. 20474034, 20774052, and 20990234), by the National Science Fund for Distinguished Young Scholars of China (No. 20925414), by the Chinese Ministry of Education with the Program of New Century Excellent Talents in Universities (Grants No. ncet-05-0221), and by Nankai University ISC. A.-C.S. gratefully acknowledges the support from the Natural Sciences and Engineering Research Council (NSERC) of Canada.

REFERENCES

(1) Abetz, V.; Simon, F. W. *Adv. Polym. Sci.* **2005**, *189*, 125–212.
(2) Bates, F. S.; Fredrickson, G. H. *Phys. Today* **1999**, *52*, 32–38.
(3) Hamley, I. W. *The Physics of Block Copolymers*; Oxford University Press: New York, 1998; p viii, 424 pp.
(4) Hadjichristidis, N.; Iatrou, H.; Pitsikalis, M.; Pispas, S.; Avgeropoulos, A. *Prog. Polym. Sci.* **2005**, *30*, 725.
(5) Hadjichristidis, N.; Iatrou, H.; Pitsikalis, M.; Mays, J. W. *Prog. Polym. Sci.* **2006**, *31*, 1068.
(6) Pitsikalis, M.; Pispas, S.; Mays, J. W.; Hadjichristidis, N. *Adv. Polym. Sci.* **1998**, *135*, 1.
(7) Hadjichristidis, N.; Pispas, S.; Pitsikalis, M.; Iatrou, H.; Vlahos, C. *Adv. Polym. Sci.* **1999**, *142*, 71.
(8) Hadjichristidis, N.; Pitsikalis, M.; Iatrou, H. *Adv. Polym. Sci.* **2005**, *2005*, 189.
(9) Hashimoto, T.; Yamasaki, K.; Koizumi, S.; Hasegawa, H. *Macromolecules* **1993**, *26*, 2895–2904.
(10) Hashimoto, T.; Koizumi, S.; Hasegawa, H. *Macromolecules* **1994**, *27*, 1562–1570.
(11) Koizumi, S.; Hasegawa, H.; Hashimoto, T. *Macromolecules* **1994**, *27*, 4371–4381.
(12) Yamaguchi, D.; Bodycomb, J.; Koizumi, S.; Hashimoto, T. *Macromolecules* **1999**, *32*, 5884–5894.
(13) Yamaguchi, D.; Shiratake, S.; Hashimoto, T. *Macromolecules* **2000**, *33*, 8258–8268.
(14) Yamaguchi, D.; Hashimoto, T. *Macromolecules* **2001**, *34*, 6495–6505.
(15) Yamaguchi, D.; Hasegawa, H.; Hashimoto, T. *Macromolecules* **2001**, *34*, 6506–6518.
(16) Yamaguchi, D.; Takenaka, M.; Hasegawa, H.; Hashimoto, T. *Macromolecules* **2000**, *34*, 1707–1719.
(17) Court, F.; Hashimoto, T. *Macromolecules* **2001**, *34*, 2536–2545.
(18) Court, F.; Hashimoto, T. *Macromolecules* **2002**, *35*, 2566–2575.
(19) Court, F.; Yamaguchi, D.; Hashimoto, T. *Macromolecules* **2006**, *39*, 2596–2605.
(20) Court, F.; Yamaguchi, D.; Hashimoto, T. *Macromolecules* **2008**, *41*, 4828–4837.
(21) Kane, L.; Satkowski, M. M.; Smith, S. D.; Spontak, R. J. *Macromolecules* **1996**, *29*, 8862–8870.
(22) Lin, E. K.; Gast, A. P.; Shi, A. C.; Noolandi, J.; Smith, S. D. *Macromolecules* **1996**, *29*, 5920.
(23) Papadakis, C. M.; Mortensen, K.; Posselt, D. *Eur. Phys. J. B* **1998**, *4*, 325–332.
(24) Vilesov, A. D.; Floudas, G.; Pakula, T. *Macromol. Chem. Phys.* **1994**, 195.
(25) Birshtein, T. M.; Liatskaya, Y. V.; Zhulina, E. B. *Polymer* **1990**, *31*, 2185–2196.
(26) Zhulina, E. B.; Birshtein, T. M. *Polymer* **1989**, *32*, 1299–1308.
(27) Zhulina, E. B.; Lyatskaya, Y. V.; Birshtein, T. M. *Polymer* **1990**, *33*, 332–342.
(28) Lyatskaya, Y. V.; Zhulina, E. B.; Birshtein, T. M. *Polymer* **1992**, *33*, 343–351.
(29) Birshtein, T. M.; Lyatskaya, Y. V.; Zhulina, E. B. *Polymer* **1992**, *33*, 2750–2756.
(30) Shi, A. C.; Noolandi, J. *Macromolecules* **1994**, *27*, 2936–2944.
(31) Shi, A. C.; Noolandi, J. *Macromolecules* **1995**, *28*, 3103–3109.
(32) Matsen, M. W. *J. Chem. Phys.* **1995**, *103*, 3268–3271.
(33) Matsen, M. W.; Bates, F. S. *Macromolecules* **1995**, *28*, 7298–7300.
(34) Matsen, M. W. *Phys. Rev. Lett.* **1995**, *74*, 4425–4428.
(35) Wu, Z.; Li, B.; Jin, Q.; Ding, D.; Shi, A. C. *Acta Polym. Sin.* **2007**, *11*, 1035–1039.

(36) Ge, H.; Wang, Z.; Li, B.; Ding, D.; Shi, A. C. *Acta Polym. Sin.* **2007**, *2*, 119–122.
(37) Wu, Z.; Li, B.; Jin, Q.; Ding, D.; Shi, A. C. *J. Phys. Chem. B* **2010**, *114*, 15789–15798.
(38) Matsen, M. W. *J. Phys.: Condens. Matter* **2002**, *14*, R21–R47.
(39) Hong, K. M.; Noolandi, J. *Macromolecules* **1981**, *14*, 727.
(40) Matsen, M. W.; Schick, M. *Phys. Rev. Lett.* **1994**, *18*, 2660–2663.
(41) Matsen, M. W. *Eur. Phys. J. E* **2009**, *30*, 361–369.
(42) Matsen, M. W. *Macromolecules* **2003**, *36*, 9647–9657.
(43) Matsen, M. W. *J. Chem. Phys.* **1996**, *106*, 2436–2448.